Preprint
UCRL-CONF-205129

Turbulence Kinetic Energy in the Oklahoma City Urban Environment

Julie K. Lundquist, Marty Leach and Frank Gouveia

This paper was submitted to the Fifth Symposium on the Urban Environment, Vancouver, Canada, August 23-28, 2004

July 2004

6.11 TURBULENCE KINETIC ENERGY IN THE OKLAHOMA CITY URBAN ENVIRONMENT

Julie K. Lundquist, Marty Leach, and Frank Gouveia

Atmospheric Science Division
Lawrence Livermore National Laboratory, Livermore, CA, 94550

1. INTRODUCTION

A major field experiment, Joint URBAN 2003 (JU2003), was conducted in Oklahoma City in July 2003 to collect meteorological and tracer data sets for evaluating dispersion models in urban areas. The Department of Homeland Security and the Defense Threat Reduction Agency were the primary sponsors of JU2003. Investigators from five Department of Energy national laboratories, several other government agencies, universities, private companies, and international agencies conducted the experiment.

Observations to characterize the meteorology in and around the urban area complemented the observation of the dispersion of SF_6, an inert tracer gas. Over one hundred three-dimensional sonic anemometers were deployed in and around the urban area to monitor wind speed, direction, and turbulence fluxes during releases of SF_6. Sonic deployment locations included a profile of eight sonic anemometers mounted on a crane less than 1 km north of the central business district (CBD). Using data from these and other sonic anemometers deployed in the urban area, we can quantify the effect of the urban area on atmospheric turbulence and compare results seen in OKC to those in other urban areas to assess the parameters typically used in parameterizations of urban turbulence.

2. DATA SOURCES

A pseudo tower (Figure 1) was constructed just north (downwind in typical summertime southerly flow situations) of the CBD. The upstream “fetch” of this tower varied with wind direction. Figure 2 depicts building heights (gridded to a 2m grid) as a function of distance from the crane for all buildings within the southerly 30 degree sector from the crane; note that spaces with no buildings are not represented on this plot. For this sector, the mean building height is approximately 13 m. The mean and maximum building heights for all sectors are seen in Figure 3. The built-up CBD, which is located south to south-east of the crane, is apparent in Figure 3. Discussion of atmospheric stability as function of upstream fetch has been presented in Lundquist et al. (2004).

Figure 1: The pseudo-tower, outlined in red, supported by a crane to the north of the pseudo-tower. The view is to the south-west. Most winds during the JU2003 experiment were from the south. (Photo courtesy of M. Leach, LLNL.)

On the crane, R.M. Young model 81000 sonic anemometers were mounted at 7.8, 14.6, 21.5, 28.3, 42.5, 55.8, 69.7, and 83.2 m above the surface. The sonic anemometers recorded data at 10 Hz throughout the experiment. For calculations of turbulent fluxes, such $u'w'$ and $v'w'$, 30-minute time series were used to ensure adequate sampling of large scale motions. Of the 11520 30-minute time periods (at all levels) examined for this study, 413 were rejected because of instrument failure. Because the pseudo-tower was supported by a large crane to the north, time periods with a mean direction between 315° (north-westerly) and 45° (north-easterly) were rejected from analysis. Using this criterion, another 1000 30-minute segments were rejected from study. In total, 10107 30-minute time series, or 87.7% of the original data, were considered.

To adjust for any tilting of the sonic anemometer, the planar-fit correction described by Wilczak et al. (2001) has been applied to the data. The data have been rotated into a right-handed natural coordinate system: the streamwise coordinate u is aligned with the mean horizontal wind; the transverse component v is perpendicular to u in the horizontal plane, and the normal component w is perpendicular to u in the vertical plane.

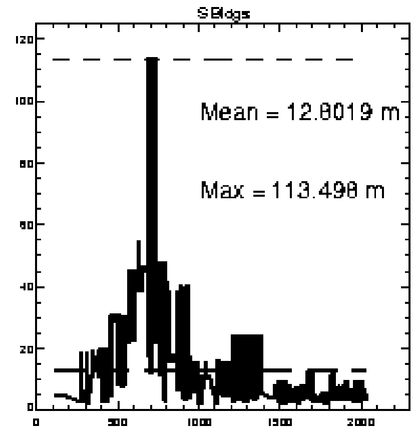

Figure 2: The variation of building height with distance from the tower for the 30 degree (165-195 degrees in meteorological coordinates) arc south of the tower.

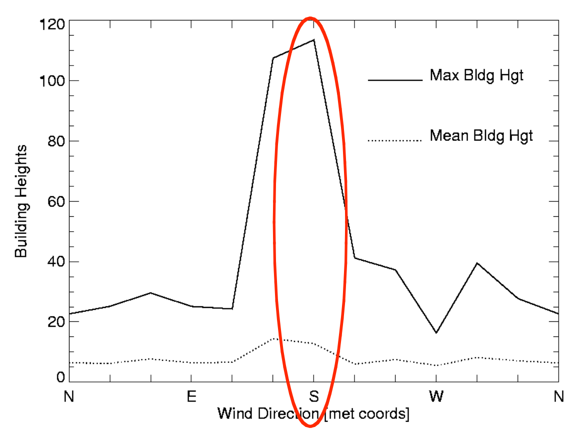

Figure 3: Variation of building heights in the fetch upstream of the tower as a function of wind direction. The mean building height varies from 5-15m, while the maximum height varies considerably. The CBD is S, SE of the crane. The red oval emphasizes data points from the 30-degree arc displayed in more detail in Figure 2.

The crane was sited just north of the CBD to ensure that most observations would be taken during periods in which the upstream fetch includes the CBD. This goal was met, as seen in Figure 4: at the crane, southerly flow was most often observed.

Other sonic anemometers were deployed throughout the city during the experiment; data from those sources will be presented in future work.

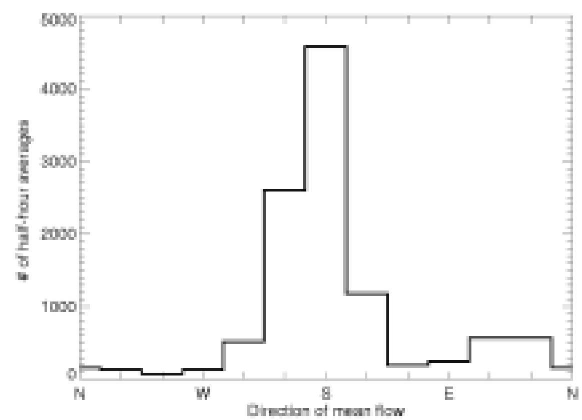

Figure 4: Histogram of wind directions observed at the crane. The flow was most often from the south, from the direction of the CBD.

3. PARAMETERIZATIONS OF URBAN TURBULENCE FOR USE IN MESOSCALE OR PUFF MODELS

Using the data from the crane pseudo-tower, we can calculate integral statistics of turbulence. By exploring their dependence on wind direction, or the height of the buildings in the upstream fetch, we can elucidate the effect of the CBD on atmospheric turbulence.

These calculations implicitly assume Monin-Obukhov similarity theory because they are non-dimensionalized by the local $u*$ measurement, where $u*$ is defined using the local turbulent fluxes:

$$u*^2 = \sqrt{\overline{u'w'}^2 + \overline{v'w'}^2} \, .$$

Summary statistics on this local friction velocity appear in Figure 5. The top panels show average profiles of $u*$ for wind directions SSW (left), S (center), and SSE (right). The dots show means, the horizontal bars indicate plus or minus one standard deviation, and the numbers indicate the number of data points included in the averages at each level. The lowest level appears to be an outlier, possibly due to the presence of a 3m tall trailer just 7 m south of the crane pseudo-tower; this structure likely dominated the fetch for the 8m sonic anemometer, and that level should not be considered when calculating general statistics.

In the lower panel of Figures 5, the variability of $u*$ with wind direction is shown. Only the top seven levels are included in this calculation, and vertical lines indicate the standard deviation. The average value for all wind directions is 0.49 ms^{-1}. As expected, a strong relationship between $u*$ and the height of upstream buildings (Figure 3) can be seen. The presence of more tall buildings increases turbulent stresses. Parameterizations of the turbulent stresses with height as a function of upstream building height will be explored in future work.

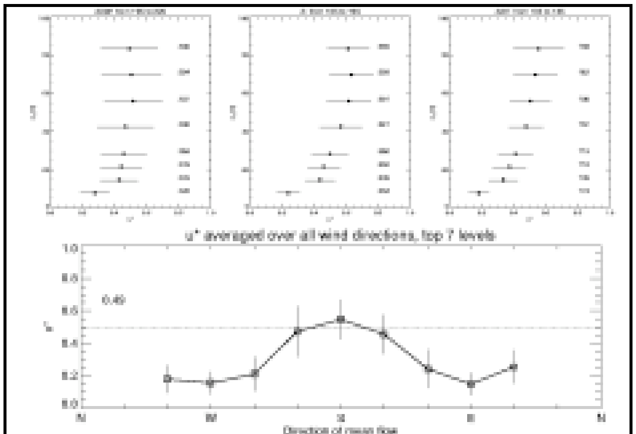

Figure 5: Variation of local turbulent stresses with height and with wind direction. See the text for more details.

3.1 *Drag Coefficient*

The relationship between the momentum flux and the mean wind speed is often used in parameterizations of turbulent stresses in numerical models. A drag coefficient, C_D may be defined such that

$$C_D = \left(\frac{u*}{U}\right)^2,$$

where U is the mean wind speed and $u*$ is the local friction velocity as defined above.

Roth (2000), based on observations from six field programs, suggests a parameterization of the drag coefficient as a function of z_H, the height of the dominant roughness elements upwind of the flow:

$$C_D^{1/2} = \frac{u*}{U} = c_1 + c_2 \exp\left(c_3 \frac{z_s}{z_H}\right),$$

where z_s is the height of the sensor measuring $u*$ and c_1, c_2, and c_3 are empirical constants, found by Roth to be 0.094, 0.353, and -0.946 respectively. Here we define z_H to be the mean height of all buildings in the upwind fetch, as seen in Figure 3.

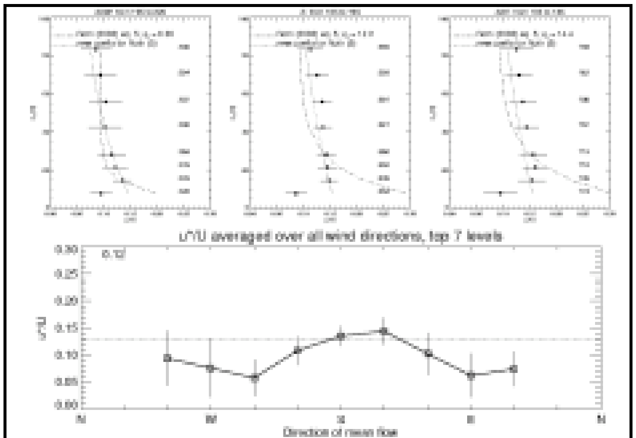

Figure 6 Drag coefficient $u*/U$ as a function of height and wind direction. See text for details.

Profiles of $C_D^{1/2}$ and comparison to Roth's parameterization are shown in Figure 6. The top panels show average profiles of $C_D^{1/2}$ for wind directions SSW (left), S (center), and SSE (right). The dots show means, the horizontal bars indicate plus or minus one standard deviation, and the numbers indicate the number of data points. As flow tended to be from the south, the statistics for the SSE, S, and SSW directions are more reliable, as evidenced by the smaller cross-bars, which denote the standard deviation of the $C_D^{1/2}$ dataset for that height and wind direction.

These observations indicate some general agreement with Roth (the dash-dot line in the profiles), especially when the flow approaches from the SSW. (Recall that the lowest level is subject to localized effects from a structure located south of the tower and should be omitted from consideration.) When constants c_1, c_2, and c_3 are recalculated based on the Oklahoma City crane data, they are found to be c_1 = 0.053, c_2 = 0.108, and c_3 = -0.116. The profiles of $C_D^{1/2}$ generated using both Roth's constants (dash-dot line) and the OKC-specific constants (dotted line) also appear in Figure 6.

In the bottom panel of Figure 6, the variation of all levels of $C_D^{1/2}$ with wind direction is shown. The averages over the top seven levels for each wind direction bin are indicated by squares, while the vertical lines indicate one standard deviation. As one would expect, the directions with rougher upwind fetch (SSW-SSE) show a higher drag coefficient.

3.2 *Normalized standard deviations*

The standard deviation (σ) of each velocity component i can be normalized with turbulent stresses:

$$A_i = \sigma_i / u*$$

These normalized velocity standard deviations are often used in parameterizations of flow within an urban boundary layer. For example, Williams and Brown (2003) define the following parameterizations for the surface stress layer:

$$\sigma_u = 2u*,$$

$$\sigma_v = 2u*, \quad \text{and}$$

$$\sigma_w = 1.3u*.$$

Roth's review of several field studies indicates that these ratios are constant with height, as might be expected within a roughness sublayer. And in fact, the Oklahoma City observations (with the exception of the aberrant lowest level) show little variation with height, as seen in the top three panels of Figure 7. Presented in Figure 7 are three mean profiles, for SSW, S, and SSE flow regimes. With the exception of the lowest level, A_u is constant with height. The dots on these plots indicate the mean value at that level, the horizontal lines indicate the mean plus or minus one standard deviation, and the numbers indicate the number of observations included in this average.

The bottom panel of Figure 7 explores the variability of A_u with wind direction, using data from the top seven levels. The most reliable statistics are for SSW, S, and SSE wind directions, which also show the lowest average value of velocity standard deviations (and the highest values of $u*$ as seen in Figure 5). The flow from these directions has experienced the large and varied roughness elements of the CBD before approaching the crane, so higher values of $u*$ are expected for these approach directions. Turbulent stresses are not as large for other approach directions, leading to higher values of A_u. This dependence on the upstream fetch is not surprising, but it should be considered in parameterizations for urban flow.

The average value of A_u is found here to be ~ 3.0, in contrast to the value of 2.0 often assumed in urban flow models (*e.g.* Williams and Brown (2003)). Similar behavior is seen for A_v., as depicted in Figure 8. The mean value of A_v is found here to be 2.7, higher than the value typically used in urban dispersion models (2.0). The behavior of A_w is seen in Figure 9, where the mean value is 1.7 rather than 1.3.

One possible explanation for these increases in normalized standard deviations in Oklahoma City, as compared to the other cities surveyed in Roth (2000), is that the observing tower here is located approximately 500m downstream of the tallest buildings in the CBD (as seen in Figure 2). The enhanced urban production of turbulent kinetic energy (and increase in $u*$) is primarily experienced by flow moving through the CBD, not by the flow downstream, in the immediate vicinity of the tower. Some TKE has likely dissipated by the time the flow reaches the tower. Therefore, $u*$ values are lower at the tower, and A_i is higher. We will test this hypothesis with data from other sonic anemometers located within the CBD.

4. SUMMARY

Data from sonic anemometers mounted at heights ranging from 8 to 73m above the surface on a crane pseudo-tower have been used to explore the characteristics of turbulence in urban Oklahoma City. As the crane was located north-northwest of the Oklahoma City central business district (CBD), and as flow during the experiment was typically southerly, the sensors on the crane observed flow in which increased turbulent kinetic energy production had been induced by the roughness elements of the Oklahoma City CBD. Under those circumstances, sensors detect higher turbulent stresses (as measured by a local friction velocity $u*$) than when the flow is from a rural or suburban area.

However, the observations presented here differ from those seen in previous work (i.e. Roth 2000). This dataset suggests higher values of velocity fluctuations (in all components, streamwise, transverse, and normal) normalized with turbulent stresses $u*$. We hypothesize that the turbulent stresses observed at the crane have already dissipated somewhat from their maximum level in the CBD because the crane is approximately 500m away from the tallest buildings in the CBD. Because $u*$and A_i are inversely proportional, this hypothesized decrease in $u*$ explains the increase in A_i.

In future work, these statistics from the crane, including TKE dissipation rate and TKE budgets, will be compared to those from sonic anemometers located within the CBD in order to more clearly elucidate the role of TKE dissipation within and downstream of a built-up urban area.

Acknowledgements

This work was performed under the auspices of the U.S. Department of Energy by the University of California, Lawrence Livermore National Laboratory under contract No. W-7405-Eng-48.

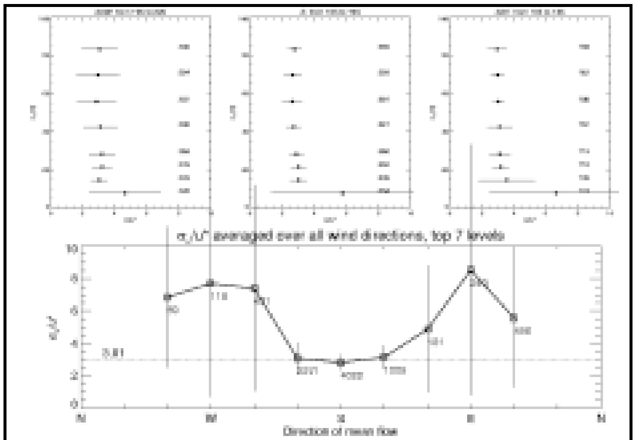

Figure 7 The standard deviation of the streamwise velocity component, normalized with local turbulent stresses. See the text for details.

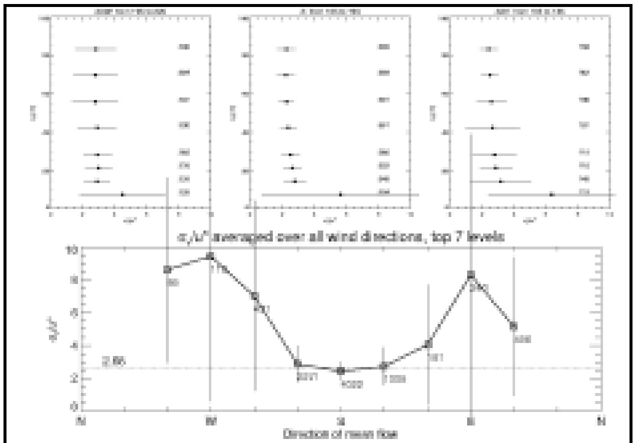

Figure 8 As in Figure 7, but for the transverse velocity component.

References

Lundquist, J. K., J. Shinn, and F. Gouveia, 2004: Observations of the turbulent kinetic energy dissipation rate in the urban environment. *Symposium on Planning, Nowcasting, and Forecasting in the Urban Zone*, Seattle, WA, 10-15 January, 2004. Available at http://ams.confex.com/ams/pdfpapers/71468.pdf

Roth, M. and T. R. Oke, 1993: Turbulent transfer relationships over an urban surface. I: Spectral characteristics. *Quart. J. Roy. Meteorol. Soc.*, **119**, 1071-1104.

Wilczak, J.M., S.P. Oncley, and S.A. Stage, 2001: Sonic anemometer tilt correction algorithms. *Bound.-Layer Meteorol.* **99**, 127-150.

Williams, M.D. and M. J. Brown, 2003: Description of the QWIC-PLUME Model. Los Alamos National Laboratory Technical Report LA-UR-03-1426. Available at http://lib-www.lanl.gov/

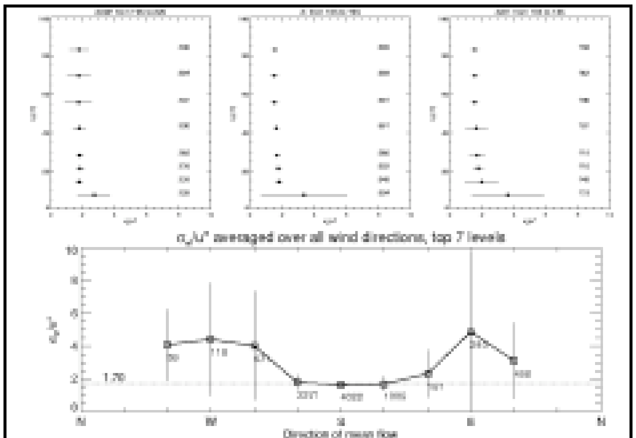

Figure 9 As in Figure 7, but for the normal velocity component.

University of California
Lawrence Livermore National Laboratory
Technical Information Department
Livermore, CA 94551